Available online at www.sciencedirect.com

ScienceDirect

IFAC PapersOnline CONFERENCE PAPER ARCHIVE

IFAC PapersOnLine 54-14 (2021) 167–172

Quantitative robustness analysis of model following control for nonlinear systems subject to model uncertainties ⋆

Julian Willkomm, Kai Wulff, and Johann Reger

Control Engineering Group, Technische Universität Ilmenau, P.O. Box 10 05 65, D-98684, Ilmenau, Germany, email: {julian.willkomm,kai.wulff,johann.reger}@tu-ilmenau.de

Abstract: We investigate a model following control (MFC) design for nonlinear minimumphase systems subject to model uncertainties. The model following control architecture is a two degrees-of-freedom structure consisting of two control loops. The model control loop (MCL) includes a nominal model of the process. The design of the process control loop (PCL) is based on the error system resulting from the nominal design and the actual process. Both control loops are designed using (partial) feedback linearisation. We analyse the robustness in view of the norm of the uncertainty and the region of attraction compared to a single-loop (partial) feedback linearisation control. It turns out that the proposed approach is able to stabilize significantly larger uncertainties, shows better tracking performance, and exhibits a larger region of attraction (based on a quadratic Lyapunov function).

Copyright © 2021 The Authors. This is an open access article under the CC BY-NC-ND license (https://creativecommons.org/licenses/by-nc-nd/4.0/)

Keywords: Model Following Control, Stability of Nonlinear Systems, Lyapunov Methods

1. INTRODUCTION

The model following control structure is a well-established control architecture that has been studied and used by practitioners for several decades, e.g. see the papers of Erzberger (1968); Ambrosino et al. (1985); Roppenecker (1990); Durham and Lutze (1991); Li et al. (1998); Skoczowski et al. (2003); Dworak et al. (2009); Osypiuk and Kröger (2010); Pajchrowski (2011); Brzózka (2012). This scheme represents a two-degrees-of-freedom structure shown in Figure 1. Essentially it consists of a process model simulated in a nominal control loop (model control loop) and a process control loop (PCL) that works on the actual process. It has been demonstrated that such control architecture is very capable in compensating disturbances and model uncertainties.

In the vast majority of publications on this topic, the model used in the model control loop (MCL) is a linearisation of the available process model leaving its approximation error for compensation via the PCL. Often the controller in the MCL and in the PCL are classical linear controllers. Only a few studies consider nonlinear approaches in the MCL or the PCL. Accordingly the robustness analysis is mostly limited to linear approaches, e.g. (Sugie and Osuka, 1993; Tsang and Li, 2001; Duan and Huang, 2008; Dworak et al., 2009; Osypiuk, 2010). Ishitobi et al. (2010) use a linear model in the MCL and an input-output linearisation approach for the PCL. Only a few studies include a nonlinear model in the MCL, e.g. (Brzózka, 2012; Huber et al., 2013; Schaper et al., 2014). Willkomm et al. (2018, 2019) let the model control loop (MCL) use a local model network (LMN), where the parameters of the linear local models are interpolated. Brzózka (2012) use a flatness-based control applied to the nonlinear model in the MCL. Nonlinear model predictive approaches are used in the case studies (Huber et al., 2013; Schaper et al., 2014). However, to the best of the authors knowledge a systematic nonlinear analysis of the potential of this approach cannot be found in the literature.

The aim of this contribution is to provide a thorough analysis of the robustness towards model uncertainties in the nonlinear system using a nonlinear model and standard nonlinear control approach in both MCL and PCL. We consider a nonlinear system in Byrnes-Isidori-form and design a standard feedback-linearisation controller for the nominal model in the MCL as well as for the resulting error dynamics. Based on a Lyapunov function for the nominal design we estimate a bound on the model uncertainty. The case study of an academic example shows that the considered MFC control structure is able to compensate much larger model uncertainties compared to single-loop feedback linearisation. The case study also shows that the region of attraction is significantly larger using this two-degrees-of-freedom architecture.

The manuscript is structured as follows. In the next section we give a formal description of the considered system class. In Section 3 we design the controller for the proposed MFC structure. Also a comparison design is described. In doing so, we analyse the bounds for the perturbation for both control architectures. An illustrative example which shows the advantages of the MFC is given in Section 4. We draw our conclusions in Section 5.

⋆ The authors kindly acknowledges support by the European Union Horizon 2020 research and innovation program under Marie Skłodowska-Curie grant agreement No. 734832.

2405-8963 Copyright © 2021 The Authors. This is an open access article under the CC BY-NC-ND license.
Peer review under responsibility of International Federation of Automatic Control.
10.1016/j.ifacol.2021.10.347

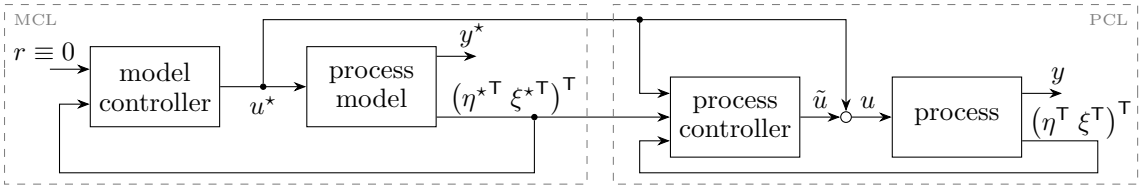

Fig. 1. Model following control (MFC) blockdiagram with model control loop (MCL) and process control loop (PCL).

2. SYSTEM CLASS AND PRELIMINARY RESULT

We consider a nonlinear minimumphase (at least locally) SISO system in normal form given by

$$\dot{\eta} = f_0(\eta, \xi) \tag{1}$$
$$\dot{\xi}_i = \xi_{i+1} \qquad \text{for } 1 \le i \le r-1 \tag{2}$$
$$\dot{\xi}_r = a(\xi, \eta) + b(\xi, \eta)u + \phi(\xi) \tag{3}$$
$$y = \xi_1 \tag{4}$$

where $\eta(t) \in \mathbb{R}^{n-r}$ and $\xi(t) \in \mathbb{R}^r$ denote the internal and external states, respectively, and $u(t), y(t) \in \mathbb{R}$ are the input and output, respectively. The relative degree is $1 \le r \le n$. The known functions $f_0 : \mathbb{R}^{n-r} \times \mathbb{R}^r \to \mathbb{R}^{n-r}$, $a : \mathbb{R}^r \times \mathbb{R}^{n-r} \to \mathbb{R}$, $b : \mathbb{R}^r \times \mathbb{R}^{n-r} \to \mathbb{R}$ and model uncertainty $\phi : \mathbb{R}^r \to \mathbb{R}$ are sufficiently smooth. Furthermore, $f_0(0,0) = 0$ and $b(\xi, \eta) \neq 0$ for all ξ and η. The model uncertainty vanishes in the origin, i. e. $\phi(0) = 0$. We assume that all states ξ and η are available for control. In case $r = n$ the internal dynamics η and (1) are dropped and the functions $a(\cdot)$, $b(\cdot)$ and $\phi(\cdot)$ only depend on ξ.

For the stability analysis we shall resort to a well-known result adapted from (Khalil, 2002).

Lemma 1. Consider the nonlinear system of the form

$$\dot{\eta} = f_0(\eta, \xi)$$
$$\dot{\xi} = A_{\mathrm{cl}}\, \xi\,,$$

where matrix A_{cl} is Hurwitz. The origin of $\left(\eta^\mathsf{T}\ \xi^\mathsf{T}\right)^\mathsf{T}$ is

- locally asymptotically stable if the origin of system $\dot{\eta} = f_0(\eta, 0)$ is asymptotically stable,
- globally asymptotically stable if the internal dynamics $\dot{\eta} = f_0(\eta, \xi)$ are input-to-state stable (ISS).

Proof. Proofs can be found in (Khalil, 2002, p. 531f). □

3. CONTROL DESIGN AND ESTIMATED REGION OF ATTRACTION

In this section we present the considered control design and compute a bound for the uncertainty ϕ based on a quadratic Lyapunov function. The control is based on the well-known model following control structure, see Fig. 1, where a nominal model runs in the model control loop (MCL). The control output obtained from the MCL is used as feedforward control for the actual process. The process control loop (PCL) caters for disturbances and model uncertainties. In our approach the nominal model in the model control loop is nonlinear and a (partial) state feedback linearisation is applied to both, the model control loop (MCL) as well as the process control loop (PCL). The design of the latter is based on the resulting error dynamics obtained from the deviation of the process with respect to the nominal model.

3.1 Model following control

For the model control loop (MCL) we design a controller using (partial) state feedback linearisation $u^\star$ and pole placement control law $v^\star$ of the form

$$u^\star = \frac{-a(\xi^\star, \eta^\star) + v^\star}{b(\xi^\star, \eta^\star)}, \qquad v^\star = -\sum_{i=1}^{r} p^\star_{i-1} \xi^\star_i\,,$$

where the parameters $p^\star_0, \dots, p^\star_{r-1} \in \mathbb{R}$ are chosen such that the polynomial

$$\lambda^r + p^\star_{r-1}\lambda^{r-1} + \cdots + p^\star_1 \lambda + p^\star_0 \tag{5}$$

is Hurwitz. This yields the closed MCL of the form

$$\dot{\eta}^\star = f_0(\eta^\star, \xi^\star) \tag{6}$$
$$\dot{\xi}^\star = A^\star \xi^\star \tag{7}$$

where $A^\star$ is a Frobenius matrix with the characteristic polynomial (5). Note that the model control loop (6)–(7) does not exhibit any uncertainties or disturbances.

For the design of the PCL we define the error states $\tilde{\eta} \coloneqq \eta - \eta^\star$ and $\tilde{\xi} \coloneqq \xi - \xi^\star$, and $\tilde{u} = u - u^\star$. The error-dynamics read

$$\dot{\tilde{\eta}} = \tilde{f}_0(\eta^\star, \tilde{\eta}, \xi^\star, \tilde{\xi})$$
$$\dot{\tilde{\xi}}_i = \tilde{\xi}_{i+1} \qquad \text{for } 1 \le i \le r-1$$
$$\dot{\tilde{\xi}}_r = \tilde{a}(\xi^\star, \tilde{\xi}, \eta^\star, \tilde{\eta}, u^\star) + b(\xi^\star + \tilde{\xi}, \eta^\star + \tilde{\eta})\tilde{u} + \phi(\xi^\star + \tilde{\xi})\,,$$

where

$$\tilde{f}_0(\eta^\star, \tilde{\eta}, \xi^\star, \tilde{\xi}) \coloneqq f_0(\eta^\star + \tilde{\eta}, \xi^\star + \tilde{\xi}) - f_0(\eta^\star, \xi^\star)$$
$$\tilde{a}(\xi^\star, \tilde{\xi}, \eta^\star, \tilde{\eta}, u^\star) \coloneqq a(\xi^\star + \tilde{\xi}, \eta^\star + \tilde{\eta}) - a(\xi^\star, \eta^\star) + (b(\xi^\star + \tilde{\xi}, \eta^\star + \tilde{\eta}) - b(\xi^\star, \eta^\star))u^\star.$$

The control law for the process controller is given by

$$\tilde{u} = \frac{-\tilde{a}(\xi^\star, \tilde{\xi}, \eta^\star, \tilde{\eta}, u^\star) + \tilde{v}}{b(\xi^\star + \tilde{\xi}, \eta^\star + \tilde{\eta})}, \qquad \tilde{v} = -\sum_{i=1}^{r} \tilde{p}_{i-1} \tilde{\xi}_i\,,$$

where the parameters $\tilde{p}_0, \dots, \tilde{p}_{r-1} \in \mathbb{R}$ are chosen such that the characteristic polynomial

$$\lambda^r + \tilde{p}_{r-1}\lambda^{r-1} + \cdots + \tilde{p}_1 \lambda + \tilde{p}_0 \tag{8}$$

is Hurwitz. This leads to the closed loop MFC dynamcis

$$\begin{pmatrix} \dot{\eta}^\star \\ \dot{\tilde{\eta}} \\ \dot{\xi}^\star \\ \dot{\tilde{\xi}} \end{pmatrix} = \begin{pmatrix} f_0(\eta^\star, \xi^\star) \\ \tilde{f}_0(\eta^\star, \tilde{\eta}, \xi^\star, \tilde{\xi}) \\ A^\star \xi^\star \\ \tilde{A}\,\tilde{\xi} \end{pmatrix} + \begin{pmatrix} 0 \\ 0 \\ 0 \\ e_r\, \phi(\xi^\star + \tilde{\xi}) \end{pmatrix} \tag{9}$$

where $e_r = (0 \ \cdots \ 0 \ 1)^\mathsf{T}$ denotes the r-th unit vector and $\tilde{A}$ is a Frobenius matrix with characteristic polynomial (8).

If $y = \xi^\star_1 + \tilde{\xi}_1 \equiv 0$, it follows $\xi^\star = -\tilde{\xi}$ and

$$y^{(r)} = 0 = e_r A^\star \xi^\star + e_r \tilde{A}\tilde{\xi} + \phi(\xi^\star + \tilde{\xi}) = e_r(\tilde{A} - A^\star)\tilde{\xi} + \phi(0)\,,$$

where $\phi(0) = 0$ holds by assumption. If the characteristic polynomials of $A^\star$ and $\tilde{A}$ are not identical, it follows that $\xi^\star = -\tilde{\xi} = 0$. So the zero-dynamics of the closed loop MFC (9) are given by

$$\begin{pmatrix} \dot{\eta}^\star \\ \dot{\tilde{\eta}} \end{pmatrix} = \begin{pmatrix} f_0(\eta^\star, 0) \\ \tilde{f}_0(\eta^\star, \tilde{\eta}, 0, 0) \end{pmatrix} \tag{10}$$

and the internal dynamics of the closed loop MFC (9) are given by

$$\begin{pmatrix} \dot{\eta}^\star \\ \dot{\tilde{\eta}} \end{pmatrix} = \begin{pmatrix} f_0(\eta^\star, \xi^\star) \\ \tilde{f}_0(\eta^\star, \tilde{\eta}, \xi^\star, \tilde{\xi}) \end{pmatrix}. \tag{11}$$

Lemma 2. The internal dynamics of the MFC (11) are ISS if and only if the internal dynamics (1) of the process (1)–(4) are ISS.

Proof.

($\Leftarrow$) If (1) is ISS, the first equation of (11)

$$\dot{\eta}^\star = f_0(\eta^\star, \xi^\star)$$

is ISS because it is simply a copy of (1) with substituted arguments. Furthermore,

$$\dot{\eta} = \dot{\eta}^\star + \dot{\tilde{\eta}} = f_0(\eta^\star + \tilde{\eta}, \xi^\star + \tilde{\xi})$$

is ISS and further it follows that

$$\dot{\tilde{\eta}} = f_0(\eta^\star + \tilde{\eta}, \xi^\star + \tilde{\xi}) - f_0(\eta^\star, \xi^\star)$$

is ISS and hence (11) is ISS.

($\Rightarrow$) Assuming that (11) is ISS. Then, the internal dynamics (1) is ISS, since the first equation of (11) is a copy of (1) only with other arguments. □

The following results provide an upper bound for the norm of the uncertainty based on quadratic Lyapunov function for the closed-loop system (9). The proof follows the analysis for perturbed systems in (Khalil, 2002).

Theorem 3. Consider the system (1)–(4) with ISS internal dynamics. The origin of the closed loop model following control (MFC) dynamics (9) is globally asymptotically stable if the uncertainty is bounded by

$$\|\phi(\xi)\|_2 < \gamma \|\xi\|_2 \tag{12}$$

with

$$\gamma < \frac{1}{(1+\sqrt{2})\|e_r^\mathsf{T} \tilde{P}\|_2}, \tag{13}$$

where $\tilde{P}^\mathsf{T} = \tilde{P} > 0$ and $\tilde{A}^\mathsf{T}\tilde{P} + \tilde{P}\tilde{A} = -I$.

Proof. We split the proof into two cases. The first case deals with full-state feedback linearisable systems ($r = n$) and the second case with partial feedback linearisable systems ($r < n$).

If $r = n$, the internal dynamics can be dropped and the MFC closed loop dynamics of (9) simplifies to

$$\begin{pmatrix} \dot{\xi}^\star \\ \dot{\tilde{\xi}} \end{pmatrix} = \begin{pmatrix} A^\star \xi^\star \\ \tilde{A}\tilde{\xi} + \phi(\xi^\star + \tilde{\xi}) \end{pmatrix}.$$

Choose the Lyapunov function candidate

$$V(\xi^\star, \tilde{\xi}) = \xi^{\star\mathsf{T}} P^\star \xi^\star + \tilde{\xi}^\mathsf{T} \tilde{P} \tilde{\xi}$$

where the symmetric and positive definite matrices $P^\star$ and $\tilde{P}$ are the solution of the respective Lyapunov equations

$$A^{\star\mathsf{T}} P^\star + P^\star A^\star = -I \tag{14}$$

$$\tilde{A}^\mathsf{T}\tilde{P} + \tilde{P}\tilde{A} = -I. \tag{15}$$

Thereby, I denotes the identity matrix of appropriate dimension (in this case $\mathbb{R}^{r\times r}$). Since $A^\star$ and $\tilde{A}$ are Hurwitz, the unique solutions for $P^\star$ and $\tilde{P}$ of (14) and (15) exist.

We calculate the derivative

$$\dot{V}(\xi^\star, \tilde{\xi}) = -\xi^{\star\mathsf{T}}\xi^\star - \tilde{\xi}^\mathsf{T}\tilde{\xi} + 2\phi(\xi^\star + \tilde{\xi}) e_r^\mathsf{T} \tilde{P} \tilde{\xi}\,. \tag{16}$$

Using the bound (12) of the uncertainty

$$\|\phi(\xi^\star + \tilde{\xi})\|_2 \le \gamma \|\xi^\star + \tilde{\xi}\|_2 \le \gamma \left(\|\xi^\star\|_2 + \|\tilde{\xi}\|_2 \right)$$

we can calculate an upper bound for the derivative of the Lyapunov function

$$\begin{aligned} \dot{V}(\xi^\star, \tilde{\xi}) \le & -\|\xi^\star\|_2^2 - \|\tilde{\xi}\|_2^2 + 2\gamma \|e_r^\mathsf{T}\tilde{P}\|_2 \|\xi^\star\|_2 \|\tilde{\xi}\|_2 \\ & + 2\gamma \|e_r^\mathsf{T}\tilde{P}\|_2 \|\tilde{\xi}\|_2^2 \\ \dot{V}(\xi^\star, \tilde{\xi}) \le & -\begin{pmatrix} \|\xi^\star\|_2 & \|\tilde{\xi}\|_2 \end{pmatrix} M \begin{pmatrix} \|\xi^\star\|_2 \\ \|\tilde{\xi}\|_2 \end{pmatrix} \end{aligned} \tag{17}$$

with

$$M = \begin{pmatrix} 1 & -\gamma \|e_r^\mathsf{T}\tilde{P}\|_2 \\ -\gamma \|e_r^\mathsf{T}\tilde{P}\|_2 & 1 - 2\gamma \|e_r^\mathsf{T}\tilde{P}\|_2 \end{pmatrix}.$$

For non-vanishing norms the derivative of V in (17) is negative if M is positive definite, i.e. the eigenvalues of M

$$\lambda_{1,2} = 1 - (1 \pm \sqrt{2})\gamma \|e_r^\mathsf{T}\tilde{P}\|_2$$

have to be positive and we require

$$\gamma < \frac{1}{(1+\sqrt{2})\|e_r^\mathsf{T}\tilde{P}\|_2}.$$

In case $r < n$, asymptotic stability of the external dynamics is established by the same reasoning as before, yielding condition (13). Since the internal dynamics of the process (1)–(4) are ISS it follows by Lemma 2 that the internal dynamics of (9) are ISS. Thus by Lemma 1 we obtain global asymptotic stability for (9). □

Remark 4. If the uncertainty bound (12) is only satisfied for some ξ in a compact neighbourhood of the origin, Theorem 3 yields local asymptotic stability within the respective region.

Remark 5. In case the zero-dynamics of the process (1)–(4) are asymptotically stable but not ISS, Theorem 3 yields local asymptotic stability of (9).

Remark 6. Choosing the identity matrix as right-hand side of the Lyapunov equations (14),(15), maximizes the inverses $\lambda_{\max}^{-1}(P^\star)$ and $\lambda_{\max}^{-1}(\tilde{P})$, (Patel and Toda, 1980).

3.2 Comparison control design

For a comparison we consider a standard single-loop (partial) feedback linearisation with

$$u = \frac{-a(\xi, \eta) + v}{b(\xi, \eta)}, \qquad v = -\sum_{i=1}^{r} p_{i-1}\xi_i\,,$$

where the parameters $p_0, \ldots, p_{r-1} \in \mathbb{R}$ are chosen such that

$$\lambda^r + p_{r-1}\lambda^{r-1} + \cdots + p_1\lambda + p_0 \tag{18}$$

is Hurwitz. This yields the closed loop dynamics

$$\dot{\eta} = f_0(\eta, \xi) \tag{19}$$

$$\dot{\xi} = A\xi + e_r \phi(\xi). \tag{20}$$

where A is a Frobenius matrix with characteristic polynomial (18). Using Lemma 1 and the assumption that the internal dynamics (1) are ISS, the origin of the closed loop

dynamics (19)–(20) are asymptotically stable if and only if the external dynamics (20) are asymptotically stable.

Choose the quadratic Lyapunov function

$$V(\xi) = \xi^\mathsf{T} P \xi\,,$$

where $P = P^\mathsf{T} > 0$ is the solution of the Lyapunov equation $A^\mathsf{T}P + PA = -I$. The derivative reads

$$\dot{V}(\xi) = -\xi^\mathsf{T}\xi + 2\phi(\xi) e_r^\mathsf{T} P \xi.$$

The same calculations as in the proof of Theorem 3 show that global asymptotic stability of the closed loop system (19)–(20) is guaranteed if $\|\phi(\xi)\|_2 < \gamma\|\xi\|_2$ with

$$\gamma < \frac{1}{2\|e_r^\mathsf{T} P\|_2}. \tag{21}$$

3.3 Discussion of the main results

The considerations leading to the result in Theorem 3 are essentially the same as for the single-loop feedback linearisation. Comparing the bounds obtained for the gain γ in (13) and (21) suggests that there is no benefit applying the MFC scheme. Note however that $\tilde{P}$ in (13) represents the Lyapunov function for the error dynamics whereas P in (21) represents the Lyapunov function for the nominal system without taking the impact of the uncertainty into account. In the MFC design we can choose $\tilde{P}$ explicitly with respect to the uncertainty. Thus it is possible to choose $\tilde{P}$ such that $\|e_r^\mathsf{T}\tilde{P}\|_2$ is minimised and therefore obtain a significantly enlarged bound on γ.

Moreover, the controller for the error dynamics is usually designed much more aggressively (compared to the nominal design) as it only acts on the error state $\tilde{\xi} = \xi - \xi^\star$, which has usually much smaller values and thus is less likely to cause large control signals. The example in the following section shows that this may significantly reduce $\|e_r^\mathsf{T}\tilde{P}\|_2$.

Observe also that the impact of the uncertainty ϕ on the derivative of the Lyapunov function in (16) vanishes as soon as $\tilde{\xi} = \xi - \xi^\star = 0$. Thus the uncertainty has very little impact on the stability of the overall system when the trajectory is close to the nominal design even though the impact of the uncertainty onto the system $\phi(\xi)$ may be large indeed.

The two degrees-of-freedom structure can also have a strong impact on the region of attraction in case the uncertainty does not satisfy (12) globally. This effect is demonstrated and quantified by the example in following section.

4. ILLUSTRATIVE EXAMPLE

Consider the second-order system from (Khalil, 2002):

$$\begin{pmatrix}\dot{x}_1\\ \dot{x}_2\end{pmatrix} = \begin{pmatrix}x_2\\ u + \phi(x)\end{pmatrix}, \qquad y = x_1$$

where the uncertainty is $\phi(x) = \beta x_2^3$ with unknown gain $\beta \geq 0$. Note that this uncertainty does not satisfy the bound (12) globally, however, we can still establish asymptotic stability locally using Theorem 3.

The model control loop (MCL) concerns the nominal system

$$\begin{pmatrix}\dot{x}_1^\star\\ \dot{x}_2^\star\end{pmatrix} = \begin{pmatrix}x_2^\star\\ u^\star\end{pmatrix}$$

and the process control loop (PCL) deals with the error dynamics

$$\begin{pmatrix}\dot{\tilde{x}}_1\\ \dot{\tilde{x}}_2\end{pmatrix} = \begin{pmatrix}\tilde{x}_2\\ \tilde{u} + \phi(x^\star + \tilde{x})\end{pmatrix},$$

where $\phi(x^\star + \tilde{x}) = \beta(x_2^\star + \tilde{x}_2)^3$.

The model controller is chosen such that the eigenvalues of the MCL are given by $\lambda_{1,2}^\star = -1 \pm j\sqrt{3}$, such that the model control equals the design of Example 9.2 in (Khalil, 2002, p. 342). The model control law is then

$$u^\star = -4x_1^\star - 2x_2^\star\,. \tag{22}$$

For the PCL, the eigenvalues are placed at $\tilde{\lambda}_{1,2} = -10$, such that the error dynamics exhibit a five times larger bandwidth compared to the nominal system. Accordingly, the process control law reads

$$\tilde{u} = -100\tilde{x}_1 - 20\tilde{x}_2\,.$$

Solving the Lyapunov equations (14)–(15) for $P^\star$ and $\tilde{P}$, respectively, yields

$$P^\star = \begin{pmatrix}\frac{24}{16} & \frac{1}{8}\\ \frac{1}{8} & \frac{5}{16}\end{pmatrix}, \qquad \tilde{P} = \begin{pmatrix}\frac{21}{8} & \frac{1}{200}\\ \frac{1}{200} & \frac{5}{198}\end{pmatrix}.$$

Note that $\|e_r^\mathsf{T}P^\star\|_2 \approx 0.3366$ and $\|e_r^\mathsf{T}\tilde{P}\|_2 \approx 0.0257$. The composed Lyapunov function reads

$$V(x^\star, \tilde{x}) = x^{\star\mathsf{T}} P^\star x^\star + \tilde{x}^\mathsf{T}\tilde{P}\tilde{x}\,. \tag{23}$$

According to Theorem 3 the uncertainty has to satisfy

$$\|\phi(x)\|_2 < \gamma\|x\|_2 \text{ with } \gamma < \frac{1}{(1+\sqrt{2})\|e_r^\mathsf{T}\tilde{P}\|_2}\,.$$

However, in our case ϕ is a cubic function of x_2. Therefore, we can only apply Theorem 3 locally by predefining a region of attraction. To obtain a parametrisation of this region of attraction we consider

$$\begin{aligned}\|\phi(x^\star + \tilde{x})\|_2 &= \beta\,|x_2^\star + \tilde{x}_2|^3 \leq \beta\,(|x_2^\star| + |\tilde{x}_2|)^3 \leq \dots\\ &\dots \leq \beta\,(|x_2^\star| + |\tilde{x}_2|)^2\,(\|x^\star\|_2 + \|\tilde{x}\|_2) \leq \dots\\ &\dots \leq \beta k^2\,(\|x^\star\|_2 + \|\tilde{x}\|_2)\end{aligned} \tag{24}$$

where $k \geq \max_{(x^\star,\tilde{x})\in\Omega}(|x_2^\star| + |\tilde{x}_2|)$, and Ω denotes the region of attraction generated by $V(x^\star, \tilde{x})$:

$$\Omega = \left\{ \begin{pmatrix}x^\star\\ \tilde{x}\end{pmatrix} \in \mathbb{R}^4 \middle| V(x^\star, \tilde{x}) \leq c \right\}$$

with $c > 0$ to be chosen, e.g. depending on the initial state.

To estimate the bound k we determine the largest value of $|x_{2,\max}^\star|$ and $|\tilde{x}_{2,\max}|$ on the level set for $V(x^\star, \tilde{x}) = c$. Differentiating V partially with respect to $x_1^\star$ and $\tilde{x}_1$ gives

$$x_{1,\max}^\star = -\frac{1}{12}x_{2,\max}^\star, \qquad \tilde{x}_{1,\max} = -\frac{1}{525}\tilde{x}_{2,\max}$$

and substitution into (23) yields

$$V(x_{\max}^\star, \tilde{x}_{\max}) = \frac{29}{96}x_{2,\max}^{\star\,2} + \frac{328}{12995}\tilde{x}_{2,\max}^2 = c.$$

Since the Lyapunov function is composed of the nominal and the error dynamics we may distinguish these influences by defining $c = c^\star + \tilde{c}$, where $c^\star > 0$ represents the nominal part and $\tilde{c} \geq 0$ the error part. Thus, we may identify

$$x_{2,\max}^{\star\,2} = \frac{96}{29}c^\star\,, \qquad \tilde{x}_{2,\max}^2 = \frac{12995}{328}\tilde{c},$$

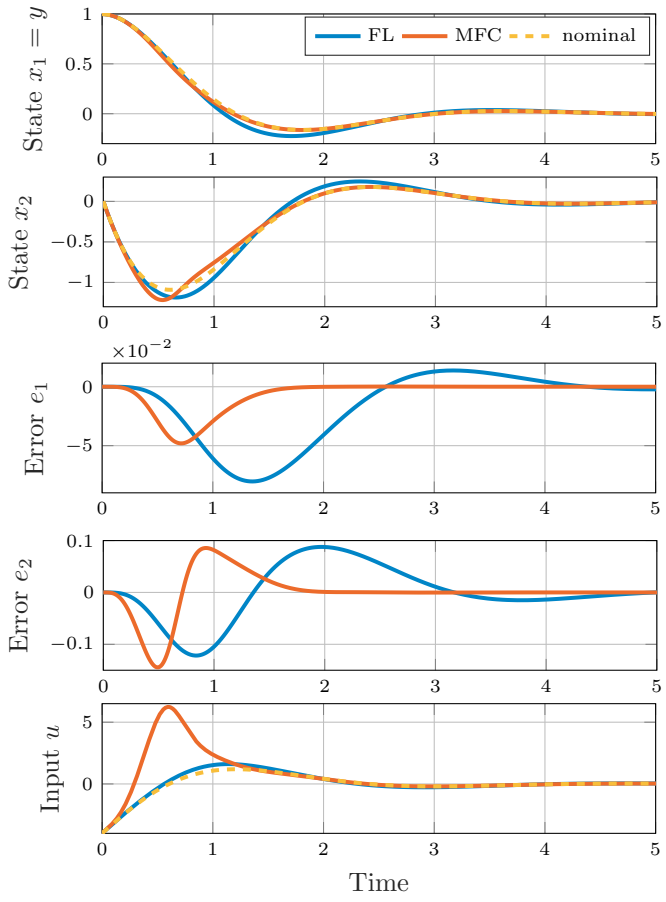

Fig. 2. Simulation of the benchmark design (blue line) with uncertainty $\beta_{\mathrm{FL}} = 0.299$ and the MFC design (red line) with $\beta_{\mathrm{MFC}} = 3.24$. The error e_i denotes the deviation of the state x_i from the nominal behaviour.

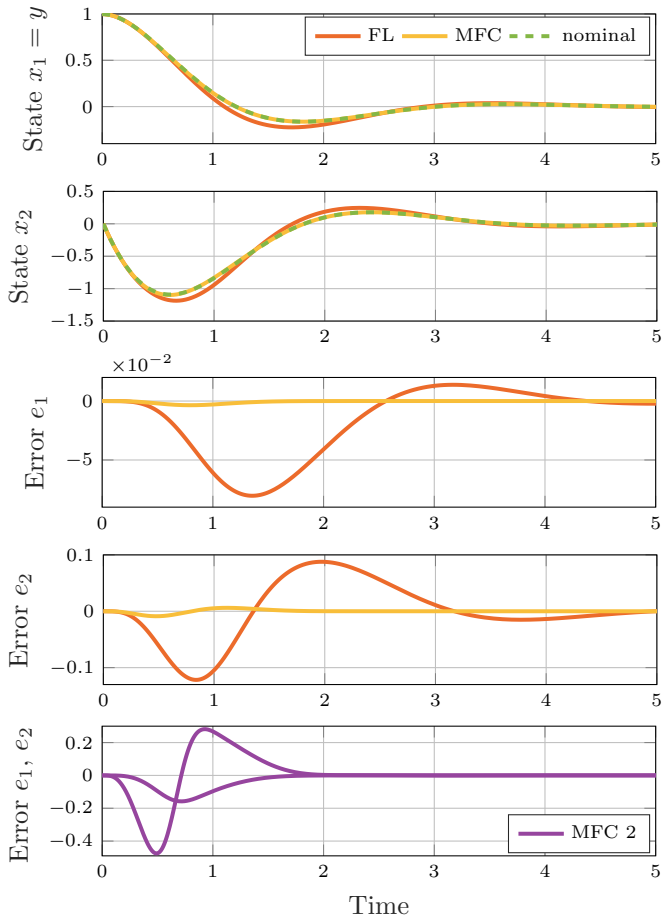

Fig. 3. Comparison for $\beta_{\mathrm{FL}} = \beta_{\mathrm{MFC}} = 0.299$. First 4 plots with initial state $x(0) = (0.9986\ 0)$, last plot only MFC with $x(0) = (3.2867\ 0)$.

and obtain

$$k = \sqrt{\frac{96}{29}c^\star} + \sqrt{\frac{12995}{328}\tilde{c}}. \tag{25}$$

We are now ready to calculate an upper bound for the uncertainty gain β evaluating (13):

$$\begin{aligned} \beta_{\mathrm{MFC}} k^2 &< \frac{1}{(1+\sqrt{2})\|e_r^{\mathsf{T}}\tilde{P}\|_2} \\ \Rightarrow\ \beta_{\mathrm{MFC}} &< \frac{1}{(1+\sqrt{2})k^2\|e_r^{\mathsf{T}}\tilde{P}\|_2} \approx 16.092\frac{1}{k^2}. \end{aligned} \tag{26}$$

For comparison we consider the single-loop feedback linearisation design in (Khalil, 2002) yielding the control law (22). Thus, we have $P = P^\star$ and the bound for the uncertainty is

$$\beta_{\mathrm{FL}} < \frac{1}{2\|e_r^{\mathsf{T}}P\|_2}\frac{1}{k_{\mathrm{FL}}^2} \approx 1.4856\frac{1}{k_{\mathrm{FL}}^2}, \tag{27}$$

Note that k_{FL} is computed as in (25), but without the extra degree of freedom obtained by the error dynamics such that $\tilde{c} = 0$.

For comparison we choose also $\tilde{c} = 0$ for the MFC design which yields exactly the same region of attraction as in the single-loop feedback linearisation. In this case the gain of the uncertainty may be roughly 10 times larger when using the proposed MFC structure compared to the benchmark design.

Figure 2 shows a simulation of both designs. The dashed line is the nominal design with no uncertainty acting. The initial state of the system is $x^\star(0) = x(0) = (0.9986\ 0)^{\mathsf{T}}$ for all simulations. For the benchmark design (blue line) we choose an uncertainty gain of $\beta_{\mathrm{FL}} = 0.299$ whereas the MFC design (red line) is exposed to an uncertainty with $\beta_{\mathrm{MFC}} = 3.24$. Both gains are chosen maximal according to (26) and (27). We observe that the MFC design is well able to compensate this considerably larger uncertainty. Moreover, the error plots show that the convergence to the nominal design occurs much faster in the MFC design (about 2 seconds instead of 4). Of course, larger control effort is needed. However, considering that the uncertainty is 10 times larger while providing comparable performance, the increase of the control signal appears moderate.

Figure 3 show simulations with equal uncertainty gains: $\beta_{\mathrm{MFC}} = \beta_{\mathrm{FL}} = 0.3$. The first four plots are simulations of the MFC design and the benchmark control with initial condition $x^\star(0) = x(0) = (0.9986\ 0)^{\mathsf{T}}$. The MFC design compensates the uncertainty remarkably well with almost identical control effort (not shown here).

For a second investigation we reverse the analysis in (26). Instead of fixing the region of attraction, we predefine a bound $\beta_{\mathrm{MFC}} = \beta_{\mathrm{FL}} = 0.3$ and consider the region of attraction obtained. Again we choose $\tilde{c} = 0$ in the MFC design for this comparison. Figure 4 shows the resulting

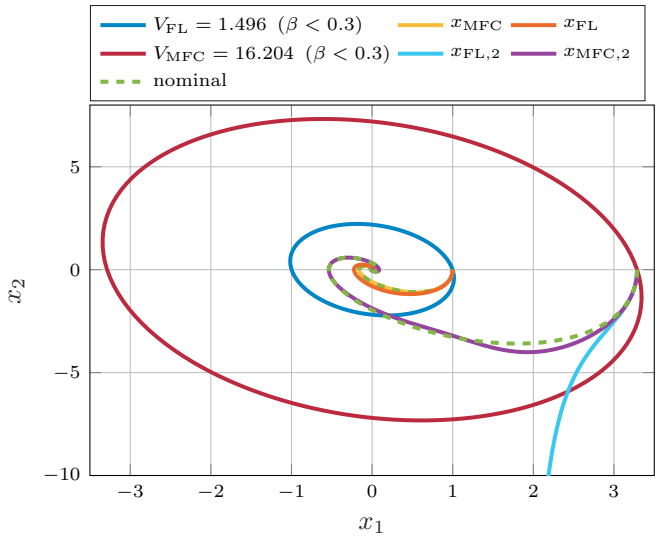

Fig. 4. Simulation in phase plane with maximum estimated region of attraction for $\beta < 0.3$ and some trajectories.

regions of attraction. The MFC design shows a much larger region of attraction (purple) compared to the benchmark design (blue).

The fifth plot in Figure 3 shows the state error for a simulation of the MFC with initial condition $x^\star(0) = x(0) = (3.2867\ 0)^\mathsf{T}$ right at the boundary of the region of attraction. While the magnitude of the error is larger due to the increase of uncertainty, the state trajectory converges to the nominal behaviour in less than 2 seconds. The simulation of the single-loop feedback linearisation (blue) with the same initial state in Figure 4 shows unstable behaviour.

5. CONCLUSION

This study provides a robustness analysis for the model following control architecture using nonlinear control methods. The analysis shows clearly the benefits of this structure and provides means to quantify its robustness properties with respect to model uncertainties. We show how these benefits of this structure can be maximised in view of robustness and also region of attraction.

REFERENCES

Ambrosino, G., Celentano, G., and Garofalo, F. (1985). Robust model tracking control for a class of nonlinear plants. *IEEE Transactions on Automatic Control*, 30(3), 275–279.

Brzózka, J. (2012). Design of robust, nonlinear control system of the ship course angle, in a model following control (MFC) structure based on an input-output linearization. *Zeszyty Naukowe Akademii Morskiej w Szczecinie*, 102(30), 25–29.

Duan, G.R. and Huang, L. (2008). Robust model following control for a class of second-order dynamical systems subject to parameter uncertainties. *Transactions of the Institute of Measurement and Control*, 30(2), 115–142.

Durham, W.C. and Lutze, F.H. (1991). Perfect explicit model-following control solution to imperfect model-following control problems. *Journal of Guidance, Control, and Dynamics*, 14(2), 391–397.

Dworak, P., Pietrusewicz, K., and Domek, S. (2009). Improving stability and regulation quality of nonlinear MIMO processes. *IFAC Proceedings Volumes*, 42(13), 180–185.

Erzberger, H. (1968). On the use of algebraic methods in the analysis and design of model-following control systems. Technical report, Washington DC.

Huber, J., Gruber, C., and Hofbaur, M. (2013). Online trajectory optimization for nonlinear systems by the concept of a model control loop – Applied to the reaction wheel pendulum. In *IEEE Conference on Control Applications*, 935–940.

Ishitobi, M., Nishi, M., and Nakasaki, K. (2010). Nonlinear adaptive model following control for a 3-DOF tandem-rotor model helicopter. *Control Engineering Practice*, 18(8), 936–943.

Khalil, H.K. (2002). *Nonlinear Systems*. Prentice–Hall, 3rd edition.

Li, G., Tsang, K.M., and Ho, S.L. (1998). A novel model-following scheme with simple structure for electrical position servo systems. *International Journal of Systems Science*, 29(9), 959–969.

Osypiuk, R. (2010). Simple robust control structures based on the model-following concept – a theoretical analysis. *International Journal of Robust and Nonlinear Control*, 20(17), 1920–1929.

Osypiuk, R. and Kröger, T. (2010). A Three-Loop Model-Following Control Structure: Theory and Implementation. *International Journal of Control*, 83(1), 97–104.

Pajchrowski, T. (2011). Robust control of PMSM system using the structure of MFC. *COMPEL - The international journal for computation and mathematics in electrical and electronic engineering*, 30(3), 979–995.

Patel, R. and Toda, M. (1980). Quantitative measures of robustness for multivariable systems. In *Joint Automatic Control Conference*, TP8–A.

Roppenecker, G. (1990). *Zeitbereichsentwurf linearer Regelungen: grundlegende Strukturen und eine allgemeine Methodik ihrer Parametrierung*. Oldenbourg.

Schaper, U., Dittrich, C., Arnold, E., Schneider, K., and Sawodny, O. (2014). 2-DOF skew control of boom cranes including state estimation and reference trajectory generation. *Control Engineering Practice*, 33(12), 63–75.

Skoczowski, S., Domek, S., and Pietrusewicz, K. (2003). Model following PID control system. *Kybernetes*, 32(5/6), 818–828.

Sugie, T. and Osuka, K. (1993). Robust model following control with prescribed accuracy for uncertain nonlinear systems. *International Journal of Control*, 58(5), 991–1009.

Tsang, K. and Li, G. (2001). Robust nonlinear nominal-model following control to overcome deadzone nonlinearities. *IEEE Transactions on Industrial Electronics*, 48(1), 177–184.

Willkomm, J., Wulff, K., and Reger, J. (2018). Feedforward control for non-minimumphase local model networks using model following control. In *IEEE Conference on Control Technology and Applications*, 1577–1582.

Willkomm, J., Wulff, K., and Reger, J. (2019). Tracking-control for the boost-pressure of a turbo-charger based on a local model network. In *IEEE International Conference on Mechatronics*, 108–113.